

30 s Response Time of K⁺ Ion-Selective Hydrogels Functionalized with 18-Crown-6 Ether Based on QCM Sensor

Zhenxiao Zhang, Qian Dou, Hongkai Gao, Bing Bai, Yongmei Zhang, Debo Hu, Ali K. Yetisen, Haider Butt, Xiaoxia Yang, Congju Li, and Qing Dai*

Potassium detection is critical in monitoring imbalances in electrolytes and physiological status. The development of rapid and robust potassium sensors is desirable in clinical chemistry and point-of-care applications. In this study, composite supramolecular hydrogels are investigated: polyethylene glycol methacrylate and acrylamide copolymer (P(PEGMA-*co*-AM)) are functionalized with 18-crown-6 ether by employing surface initiated polymerization. Real-time potassium ion monitoring is realized by combining these compounds with quartz crystal microbalance. The device demonstrates a rapid response time of \approx 30 s and a concentration detection range from 0.5 to 7.0×10^{-3} m. These hydrogels also exhibit high reusability and K⁺ ion selectivity relative to other cations in biofluids such as Na⁺, NH₄⁺, Mg²⁺, and Ca²⁺. These results provide a new approach for sensing alkali metal ions using P(PEGMA-*co*-AM) hydrogels.

I. Introduction

Potassium plays an important role in most biological processes including nerve transmission, maintenance of muscular strength, enzyme activation, and blood pressure regulation.^[1,2] Normal extracellular potassium concentration is maintained within a relatively stable range from 3.5×10^{-3} to 5.5×10^{-3} m.^[3] However, physiological disorders and diseases may lead to an abnormal potassium ion concentration, which can be fatal.^[4] For example, in the event of natural disasters (i.e., earthquakes and mine-stope collapses), injured individuals may suffer from

crush syndrome as a result of prolonged limb compression.^[5] Hyperkalemia, the most common complication of crush syndrome, is the major cause of mortality in patients.^[6] Indeed, a high potassium concentration in the blood can lead to cardio-toxicity and fatal arrhythmias.^[7] Hence, rapid detection of high potassium concentration in the blood is essential for treating wounded individuals. Potassium monitoring is also of great interest in point-of-care diagnostics and is routinely used in the hospital intensive care units (ICUs), where high potassium concentrations ($>7.0 \times 10^{-3}$ m) in serum can lead to cardiac arrests and even death.^[8-10] It is also an important parameter in predicting the occurrence of infarcts.^[8] Rapid, real-time,

and continuous measurement of potassium ion concentration is crucial when patients are monitored in physiological ranges.

Crown ether is a cavity-containing supramolecule with $\text{CH}_2\text{CH}_2\text{O}$ as the repeating unit.^[11] It is extensively used in electrochemical ion detection due to its high selectivity and affinity toward alkali metal ions.^[12] Previous studies on crown ether derivatives have mainly been focused on developing electrochemical and optical approaches for detecting potassium ions. Schuwer and Klok used surface-initiated atom transfer radical polymerization to create crown-ether-functionalized polymer brushes based on quartz crystal microbalance

Z. X. Zhang, Q. Dou, B. Bai, Dr. D. B. Hu, Prof. X. X. Yang,
Prof. Q. Dai

Division of Nanophotonics
CAS Center for Excellence in Nanoscience
National Center for Nanoscience and Technology
Beijing 100190, P. R. China
E-mail: daiq@nanoctr.cn

Z. X. Zhang
College of Material Science and Engineering
Beijing Institute of Fashion Technology
Beijing 10029, China

H. K. Gao, Y. M. Zhang
The Armed Police General Hospital
Beijing 100039, China

Prof. A. K. Yetisen
Harvard Medical School and Wellman Center for Photomedicine
Massachusetts General Hospital
65 Landsdowne Street, Cambridge, MA 02139, USA

Prof. H. Butt
Harvard-MIT Division of Health Sciences and Technology
Massachusetts Institute of Technology
Cambridge, MA 02139, USA

Prof. H. Butt
University of Birmingham
Birmingham B15 2TT, UK

Prof. C. J. Li
Beijing Institute of Nanoenergy and Nanosystems
Chinese Academy of Sciences
National Center for Nanoscience and Technology (NCNST)
Beijing 100083, P. R. China

(QCM)-D to detect potassium ions.^[13] The response time in these studies was ≈ 1 h and the total frequency shift was 10 Hz per mM at the third harmonic resonance frequency. Jarolimová et al. developed a nanosphere matrix functionalized 18-crown-6 ether in an optode form for potassium sensing with a $0.1\text{--}10.0 \times 10^{-6} \text{ mM}$ detection range.^[14] Yu et al. synthesized a linear copolymer, poly (*N*-isopropylacrylamide-*co*-benzo-15-crown-5-acrylamide), as an indicator to observe potassium ions by optical transmittance.^[15] This method was aimed at producing a portable diagnostic device. However, the response time, sensitivity, detection range, and reusability all hinder the sensor's performance. Therefore, studies on rapid, real-time, and reusable detection of physiological potassium ion concentrations are highly desirable.

Hydrogels can be functionalized with chelating agents to specifically respond to external stimuli.^[16] Moreover, supramolecular hydrogels can effectively enhance the sensitivity and selectivity for specific environmental conditions and target ions.^[12c,17] For example, 18-crown-6 ether is a suitable recognition unit for potassium ions.^[18] The outstanding mechanical properties of polyacrylamide and polyethylene glycol methacrylates (PEGMAs) can also effectively block biological macromolecules.^[19,20] Bearing these factors in mind, we synthesized copolymer hydrogels through surface-initiated polymerization using three different monomers: acrylamide, PEGMA, and (2)-allyloxymethyl 18-crown-6-ether. This method allows the hydrogel to covalently bond to the crystal plate, which can effectively improve the electrode life.^[21] By adjusting the monomer ratio, the detection range can cover the physiological range of K^+ ion concentrations. The thickness of the hydrogel film was near 165 nm, which could simultaneously reduce the response time and meet the detection requirements. The QCM sensor was highly sensitive, fast, stable, and was able to detect the sub-nanometer mass changes in the biosensors.^[22] With the development of QCM technology in the liquid phase, QCM sensors are increasingly used for the detection of biological fluids.^[23] In addition, we use hydrogel as the detection material as it has certain viscoelasticity. The best feature of QCM is that it provides interesting ways to characterize the mass and viscoelastic properties of complex thin biopolymeric films.^[24] The QCM sensor was also selected to realize real-time analyte detection.^[25] Hence, we measured the hydrogel performance using a quartz crystal microbalance, and these novel supramolecular hydrogels displayed a rapid and sensitive response to K^+ ions. The hydrogel films maintained their reversibility in aqueous conditions. They also exhibited higher selectivity to K^+ ions compared to other metal ions, such as Na^+ , NH_4^+ , Mg^{2+} , and Ca^{2+} .

2. Synthesis and Characterization

The 18-crown-6 ether functionalized hydrogel films were immobilized onto a quartz crystal by surface-initiated polymerization (Figure 1a-d). The quartz crystal was first cleaned by Piranha solution (Figure 1a).^[26] Afterward, the crystal was modified with (3-aminopropyl) triethoxysilane (APS) to graft active amino groups ($\text{t}^{\prime}\text{NH}_2$)^[27] (Figure 1b), followed by an amino-maleic anhydride ring-opening reaction.^[28] The latter reaction was undertaken so that the surface of the quartz crystal was

grafted with polymerizable carbon–carbon double bonds ($\text{C}\equiv\text{C}$) (Figure 1c). Finally, the prepolymer solution was coated on the modified quartz crystal surface and spin-coated to form a homogeneous liquid layer. The 18-crown-6 ether functionalized composite supramolecular hydrogels were synthesized using UV-initiated free-radical polymerization (Figure 1d).

A schematic of the hydrogel structure is shown in Figure 1e with polyacrylamide and polyethylene glycol methacrylate as the main chain and 18-crown-6-ether as the pendant group, formed by the copolymerization of acrylamide, polyethylene glycol methacrylate, and (2)-allyloxymethyl 18-crown-6-ether. Figure 1f shows the K^+ ion-recognition processes for the hydrogel films. This reaction was reversible in aqueous conditions.^[13,29] The combination of K^+ with the 18-crown-6 ether is a 1:1^[30] ratio, where K^+ forms a coordinate bond with the oxygen atom on the 18-crown-6 ether.

3. Results and Discussion

Atomic force microscopy (AFM), scanning electron microscopy (SEM), and differential scanning calorimetry (DSC) were used to investigate the homogeneity, mechanical properties, and morphology of the hydrogel films. The AFM results showed that the thickness of the hydrogel was roughly 165 nm (Figure 2a). We can control the film thickness via the rotation speed of spin coating; the results are shown in Figure S1 (Supporting Information). From the experimental results, we can see that the thickness of the hydrogel film reduced linearly as the rotational speed increased. According to various performance requirements, we can adjust the speed to achieve the optimized thickness of the hydrogel film. The hydrogel surface morphology was measured by AFM. The hydrogel surface was homogeneous (peak-valley roughness $\approx 21 \text{ nm}$) and displayed several irregular holes 100–250 nm in diameter (Figure 2b). The glass transition temperature (T_g) was also measured by DSC to investigate the polymer's mechanical properties. T_g (64.87°C) was higher than the temperature range of the human body (Figure 2c). In this manner, the hydrogel can maintain its characteristic properties within the normal temperature range of the human body. The cross-sectional morphology of the freeze-dried hydrogels was examined by SEM, which indicated a porous structure (Figure 2d). These images suggest a large surface area for the hydrogel, which can effectively increase reaction rate kinetics between K^+ ions and the 18-crown-6 ether complexation in the hydrogel.

Fourier transform infrared spectroscopy (FTIR), contact angle measurements, and AFM imaging were conducted on the hydrogel films grown on quartz crystals. The FTIR spectra are shown in Figure 3a. The FTIR spectra of quartz crystal without any treatment is the black curve (Figure 3a-i), as the cleaned quartz crystal surface exhibited a peak at $\approx 925 \text{ cm}^{-1}$ (the red curve Figure 3a-ii). This absorption peak can be attributed to $\text{t}^{\prime}\text{OH}$ bond stretching. In Figure 3a-iii, the quartz crystal was modified with APS, and the absorption peak at $\approx 1680 \text{ cm}^{-1}$ corresponds with $\text{t}^{\prime}\text{NH}_2$. In the fingerprint region, $\text{t}^{\prime}\text{N}$ bond stretching is located at $\approx 1262 \text{ cm}^{-1}$ and $\text{Si}^{\prime}\text{O}^{\prime}\text{C}$ bond stretching at $\approx 968 \text{ cm}^{-1}$. In Figure 3a-iv, the quartz crystal treated by maleic anhydride displayed a peak at $\approx 1650 \text{ cm}^{-1}$,

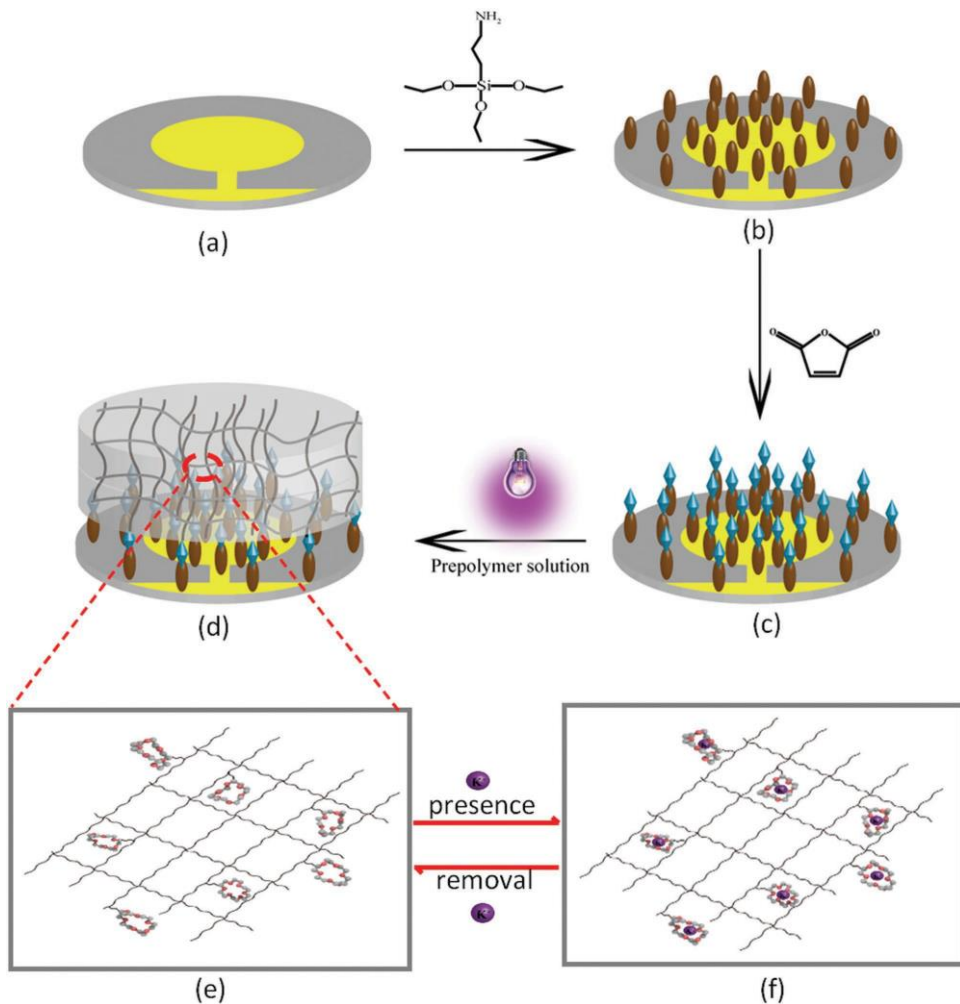


Figure 1. Procedure for the synthesis of crown-ether functionalized hydrogel films, grown on quartz crystals, and the structures and K⁺ ion-recognition properties of the hybrid hydrogels. a) The quartz crystal was cleaned by Piranha solution. b) The quartz crystal was modified with (3-aminopropyl) triethoxysilane (APS). c) The quartz crystal was grafted with a polymerizable carbon–carbon double bond (C=C). d) The quartz crystal coated by 18-crown-6 ether functionalized composite supramolecular hydrogels. e) Structures of the hybrid hydrogels and f) K⁺ ion-recognition property.

which is due to C=C bond stretching. In Figure 3a-v, the coated hydrogel exhibited C=C and C=O stretching, a strong absorption peak at ≈ 1100 cm⁻¹ and a low intensity band at ≈ 1726 cm⁻¹, respectively. The results of the FTIR measurements indicate that the target substances of each step were successfully grafted onto the quartz crystal surface.

The hydrophilicity of the quartz crystal surface was also studied in different steps using contact angle measurements. The shapes of the water drops on the surface of the untreated quartz crystal displayed a contact angle of 81.3° (Figure 3b). Correspondingly, the water contact angle of the quartz crystals decreased by ≈ 10 ° with each step of the experiment. This trend accounts for a decrease in the water contact angle from 81.3° to 54.2°, demonstrating that the surface hydrophilicity of the quartz crystal increased in each step of the experiment. This was also supported by AFM measurements (Figure 3c), which revealed that the untreated quartz crystal's surface roughness was less than ≈ 2 nm (Figure 3c-i). After the quartz crystal was treated with piranha solution, the surface roughness increased

to ≈ 5 nm (Figure 3c-ii). A depression in the surface was observed due to etching of the piranha solution on the quartz crystal. The quartz crystal roughness increased to ≈ 20 nm after being treated with APS (Figure 3c-iii). Finally, after treatment with maleic anhydride, the surface roughness increased to ≈ 25 nm (Figure 3c-iv).

The sensitivity, reusability, and selectivity of the 18-crown-6 ether functionalized hydrogel films were investigated based on a QCM sensor to identify K⁺ ions (Figure 4). The stability of the QCM sensor was first tested. The QCM sensor revealed high stability with several frequency shifts over 200 min in a potassium chloride aqueous solution (3×10^{-3} M) (Figure 4a). These frequency shifts were no greater than 2.7 Hz. We also extended the test time to 48 h, the results are shown in Figure S2 (Supporting Information). We can find that the QCM sensor frequency shift was 4.36 Hz within 48 h (the fundamental frequency of this QCM system is 5×10^6 Hz, only 0.87 ppm of the fundamental frequency). This demonstrates the good stability of our QCM sensor.

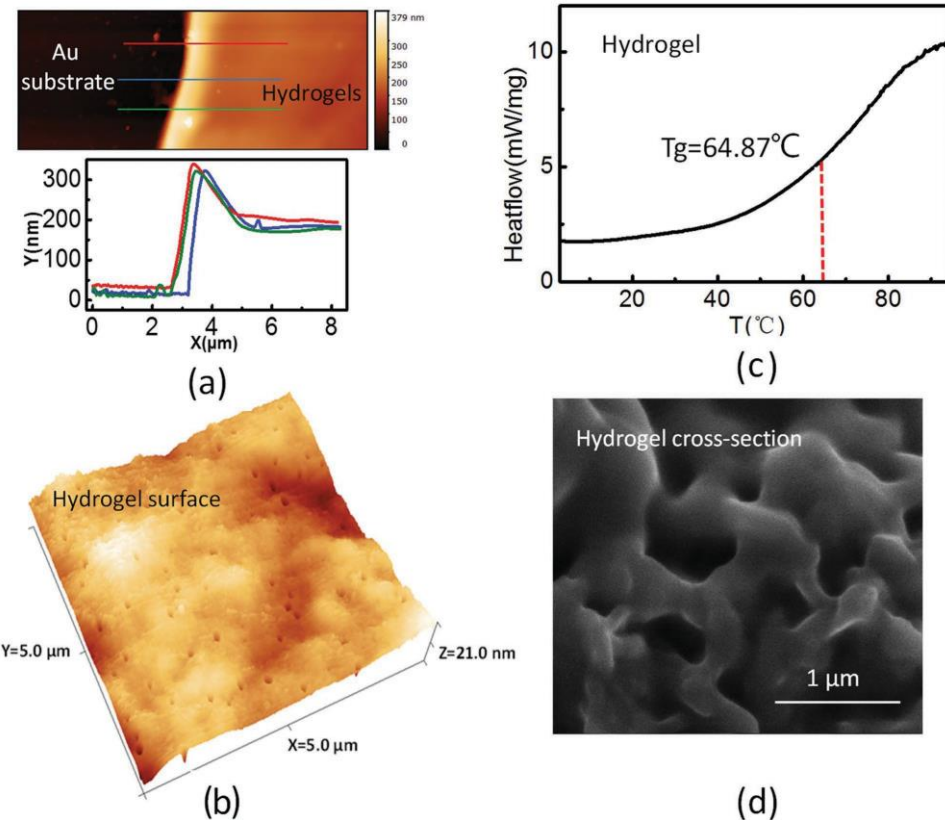


Figure 2. The homogeneity, mechanical properties, and morphology of the hydrogel film. a) Thickness of the hydrogel thin film. b) AFM image of the hydrogel surface morphology. c) DSC curves of the hydrogels. d) SEM image of the hydrogel's cross-section morphology.

The reaction of the 18-crown-6-ether functionalized hydrogels films was measured in response to K^+ ions. Figure 4b shows the QCM sensor in response to changes in the K^+ ion concentration. With an increase in potassium chloride (KCl) concentration, the frequency gradually decreased. The detection range was from 0.5×10^{-3} to 7.0×10^{-3} m, which covered the physiological K^+ concentration. When the K^+ concentration increased to 7.0×10^{-3} m, the total frequency shifted by 100 Hz. We identified the lowest concentration of potassium ion solution that can be detected by our system and the results are shown in Figure S3 (Supporting Information). We can see that when the solution concentration is 0.3×10^{-3} m, the 18-crown-6 ether functionalized hydrogel films begins to respond with a frequency shift of 3.0 Hz. Therefore, our QCM sensor has a detection limit of 0.3×10^{-3} m.

Figure 4c reveals that the response time of each 1.0×10^{-3} m K^+ ion increment examined was rapid (~ 30 s) and comparable with previously reported data.^[31] We performed an experiment to study the effect of hydrogel films with different thicknesses on response time. We tested the response time of 18-crown-6 ether functionalized hydrogel films with different thicknesses to 4×10^{-3} m KCl solution. The film thicknesses were 56, 95, 127, and 165 nm, respectively. The results are shown in Figure S4 (Supporting Information). From our experimental results, the thickness of the hydrogel has no conspicuous effect on the response time within a certain range. The cause of this result may be determined by the properties and structure of the

hydrogel. First, hydrogel is a network of hydrophilic polymer chains interwoven, which can dramatically response to environmental stimuli.^[31] Second, due to the Figure 2b,d, we found that the structure of the hydrogel was porous; the pore size was within 100–250 nm. This indicated that the surface area of the hydrogel film was relatively large, which could effectively increase diffusion rate when the K^+ ion-containing aqueous solution was introduced to the hydrogel. These characteristics of the hydrogel result in the response time not related to the film thickness within a certain range.

In order to quantify the relationship between membrane thickness (T) and the response frequency shift (Δf), we did an experiment as shown in Figure S5 (Supporting Information). It was observed that the response frequency shifts of the hydrogel films in 4×10^{-3} m KCl solution is increased as the film thickness raised from 56 to 165 nm. This is because the thicker the hydrogel film is, the more potassium ions can be combined with 18-crown-6 ether, which then lead to higher sensitivities.

The frequency difference exhibited a linear relationship with the K^+ ion concentration (Figure 4d). The reproducibility of the K^+ ion-selective electrode was also measured. Figure 4d shows the test results of three samples, in which the linear range varied from 0.5×10^{-3} to 7.0×10^{-3} m. The coefficient of variation was below 7%, well within the acceptable range. These data indicate that the potassium ion-selective electrode results are reproducible. As the instrument model we use is SRS QCM-200, the resistance represents the dissipation.^[32]

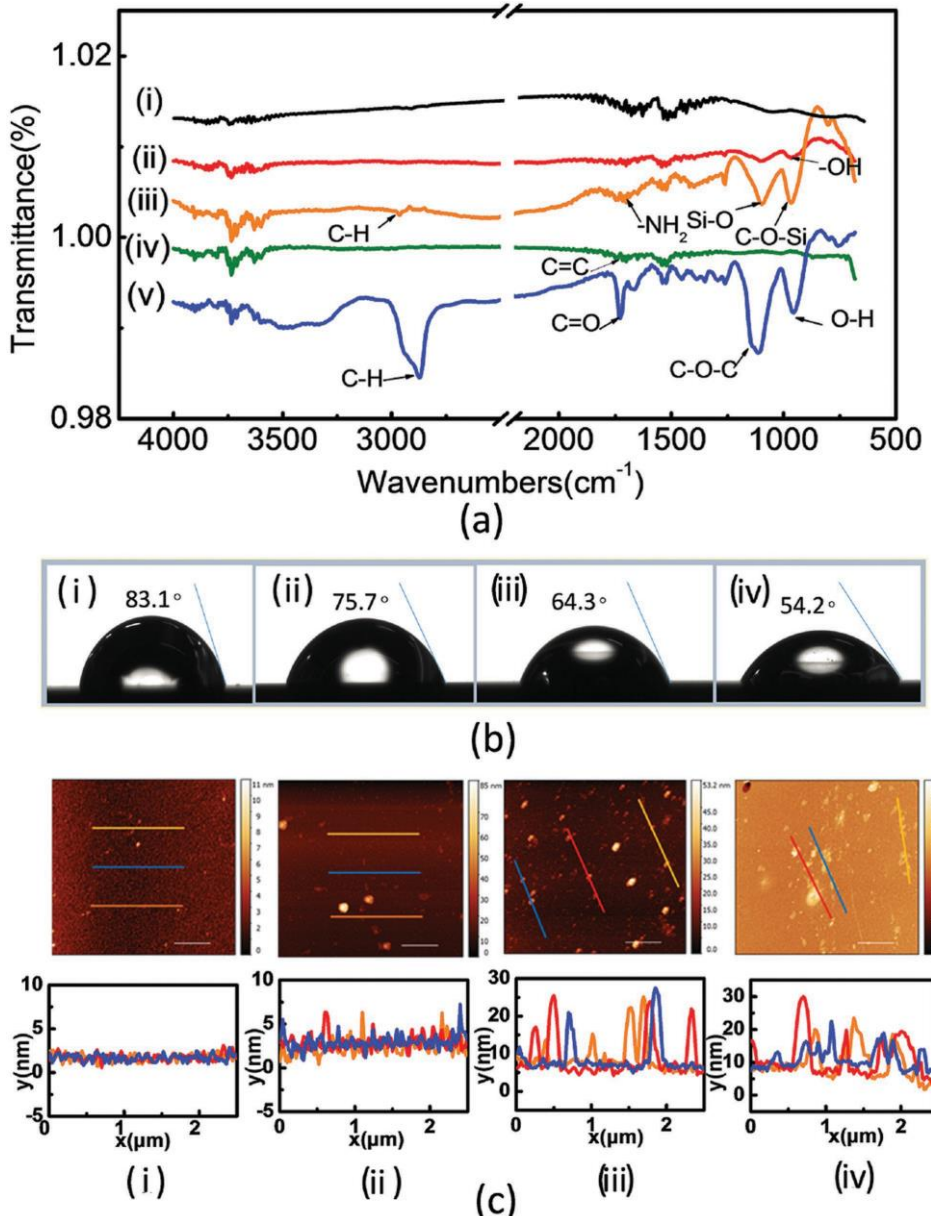


Figure 3. a) FTIR, b) contact angle measurements, and c) AFM images of the quartz crystal surface at different pretreatment steps: the quartz crystal (i) without any treatment; (ii) was cleaned by Piranha solution; (iii) modified with (3-aminopropyl) triethoxysilane (APS); (iv) modified with maleic anhydride; and a-v) the FTIR of the quartz crystal surface coated with 18-crown-6 ether functionalized composite supramolecular hydrogels.

The concentration–resistance curve is shown in Figure S6 (Supporting Information). From the experimental results, we can see that with the increase of potassium concentration, the resistance increases gradually. There is a linear relationship between the logarithm of potassium ion concentration and the change of resistance within our test concentration range. This proves that the dissipation is linearly related to the logarithm of the concentration within our test concentration range. The results of the reversibility test of the 18-crown-6-ether functionalized hydrogel film coated QCM chip are shown in Figure 4e. The hydrogel films maintained their reversibility by alternately introducing deionized water and KCl ($3.0 \times 10^{-3} \text{ M}$) solutions in 10 cycles.

The selectivity of the 18-crown-6 ether functionalized hydrogel films toward K⁺ ions was 14–50 times higher compared with other metal ions (Mg²⁺, Ca²⁺, Na⁺, NH₄⁺) (Figure 4f). At a concentration of $6 \times 10^{-3} \text{ M}$, the other cations did not cause significant frequency shifts. This suggests that the hydrogel films are selective to K⁺ ions.

4. Conclusions

We have successfully synthesized a K⁺ ion-selective P(PEGMA-*co*-AM) hydrogel functionalized with 18-crown-6-ether based on a QCM sensor using surface-initiated polymerization. The

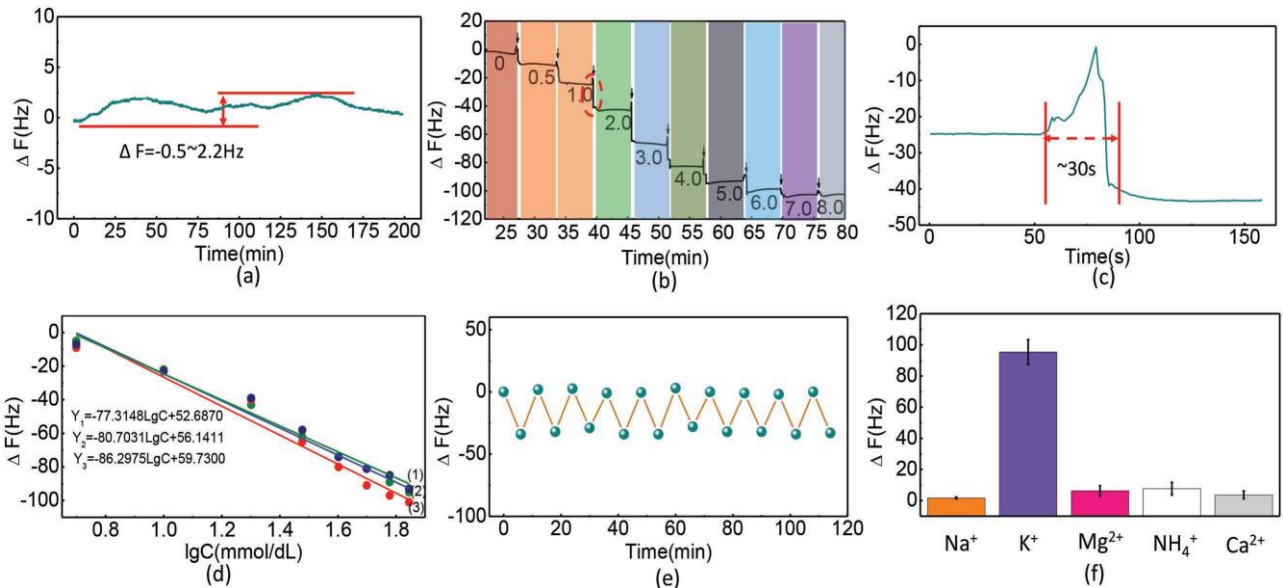


Figure 4. The sensitivity, reusability, and selectivity of 18-crown-6 ether functionalized hydrogels films based on a QCM sensor to identify K⁺ ions. a) Frequency shift over 200 min in 3×10^{-3} M KCl solution. b) The 18-crown-6-ether functionalized hydrogel film coated on a QCM chip in response to various KCl concentrations. c) Enlarged image of the red area (b). d) Fitted curve depicting the change in frequency shift and the logarithm of KCl concentration. e) Reversibility of the 18-crown-6-ether functionalized hydrogel films coated on a QCM chip. f) Comparison of the resonance frequency shift of the 18-crown-6-ether functionalized hydrogel films to 6.0×10^{-3} M solutions of different monovalent and divalent metal ion solutions.

hydrogels exhibited rapid response and high selectivity to K⁺ ions when compared with other cations, such as Na⁺, NH₄⁺,

Mg²⁺, and Ca²⁺. The detection range for K⁺ sensing varied from 0.5×10^{-3} to 7.0×10^{-3} M, covering the physiological concentration range. More importantly, the hydrogel revealed potential reusability. To the best of our knowledge, this investigation is the first demonstration of 18-crown-6-ether functionalized P(PEGMA-co-MA) hydrogels to detect K⁺ ions in aqueous solution. Furthermore, by choosing different chelating agents, this hydrogel network could be used in the preparation of a wide range of other host-guest detection systems for quantitatively sensing biomarkers in clinical samples.

5. Experimental Section

Materials: Acetone, ethanol, hydrogen peroxide 30%, sulfuric acid, dimethyl formamide, and dimethyl sulfoxide were purchased from Beijing Chemical Works. (3-Aminopropyl) triethoxysilane (Alfa Aesar), maleic anhydride (Sinopharm Chemical Reagent Co., Ltd), and N,N'-methylene-bis-acrylamide were used as the crosslinking agent for the hydrogel synthesis. 2,2-Dimethoxy-2phenylacetophenone (Tokyo Chemical Industry) and 2-(allyloxymethyl) 18-crown-6-ether were used as the detection units. Polyethylene glycol methacrylate (PEGMA $M_n = 500$) (Sigma Aldrich) and acrylamide (Xilong Scientific Co., Ltd.) were used as the skeleton structure, and PEGMA as the effect of blocking the biological macromolecules. The purity of all the chemicals was greater than 98%, unless stated otherwise.

Characterization: The hybrid hydrogels were characterized by atomic force microscopy using Neaspec s-SNOM. The cross-sectional morphology was measured by scanning electron microscopy (Hitachi S-4800), and the samples were freeze-dried and brittle fractured in liquid nitrogen before testing to obtain a smooth section. DSC

curves were obtained using a DSC8500, where the heating rate was set to $10 \text{ }^{\circ}\text{C min}^{-1}$.

FTIR Microscopy Measurements: Infrared transmission measurements

were performed using an FTIR microscopy (Thermo Fisher Nicolet iN10). A background spectrum was generated for each measurement. An untreated quartz crystal was used to extract the background signal. Each measurement was repeated three times to confirm the transmitted spectrum. The water contact angle was measured using a KRUSS DSA100, in which each sample was tested three times to determine the average. Quartz crystal microbalance measurements were carried out using an SRS-QCM 200 (fundamental frequency of 5 MHz), where the injection volume of potassium chloride was 600 μL , and the pump flow rate was set to 2 mL min^{-1} .

Fabrication of K⁺ Ion-Selective Electrode: Before plating the polymer film, quartz crystals were pretreated. First, the quartz crystals were sonicated for 30 min in ethanol and acetone, and dried under nitrogen, respectively. Then the quartz crystals were sonicated in a piranha solution (98% H₂SO₄:30% H₂O₂ = 7:3) for 10 min to eliminate organic substances, rinsed with deionized water, and dried under nitrogen.

The quartz crystals were incubated for 12 h in a 30 mL mixed solution in which the APS and ethanol volume ratio was 1:200 to graft active amino groups (t-NH_2). Following that, the quartz crystals were rapidly dried under nitrogen to prevent the APS from hydrolyzing in the air. They were then placed in a 30 mL DMF solution containing 2% maleic anhydride for 24 h and dried under nitrogen to graft the double bond.

Finally, 30 μL of prepolymer solution droplets was placed on the quartz crystal with a spin coater at a spinning speed of 4500 rpm so that the prepolymer solution could form a uniform coating on the quartz crystal. The hybrid hydrogels (P(PEGMA-AM)) functionalized with 18-crown-6-ether were synthesized by UV-initiated polymerization. The quartz crystal was then placed into the UV Cryo Chamber at 365 nm for 30 min.

Preparation of Prepolymer Solution: N,N'-methylene-bis-acrylamide (5.02 mg), 2,2-dimethoxy-2phenylacetophenone (2.5 mg), acrylamide (20 mg), 2-(allyloxymethyl) 18-crown-6-ether (15 mg), and PEGMA (10 mg) were dissolved in dimethyl sulfoxide (100 μL). The solution was stirred under 24 $^{\circ}\text{C}$ for 12 h.

Quantification of Metal Ions: The QCM was first stabilized in deionized water, and then tested in deionized water without potassium ions. The frequency was recorded as F_0 . Different concentrations of potassium ion solutions were recorded as F_1 and $F_1 - F_0$ with their corresponding frequency shifts.

Supporting Information

Supporting Information is available from the Wiley Online Library or from the author.

Acknowledgements

The National Key Research and Development Program of China (Grant No. 2016YFA0201600), the National Natural Science Foundation of China (Grant Nos. 51372045, 11504063, 11674073), and the key program of the bureau of Frontier Sciences and Education Chinese Academy of Sciences (QYZDB-SSW-SLH021).

Conflict of Interest

The authors declare no conflict of interest.

Keywords

potassium detection, QCM sensors, supramolecular hydrogels

- [1] a) F. He, Y. Tang, S. Wang, Y. Li, D. Zhu, *J. Am. Chem. Soc.* **2005**, *127*, 12343; b) B. Kim, I. H. Jung, M. Kang, H. K. Shim, H. Y. Woo, *J. Am. Chem. Soc.* **2012**, *134*, 3133.
- [2] A. Sigel, H. Sigel, R. K. Sigel, *The Alkali Metal Ions: Their Role for Life*, Springer, Berlin **2016**.
- [3] S. A. Lanham-New, H. Lambert, L. Frassetto, *Adv. Nutr.* **2012**, *3*, 820.
- [4] O. S. Better, Z. A. Abassi, *Nat. Rev. Nephrol.* **2011**, *7*, 416.
- [5] Q. He, F. Wang, G. Li, X. Chen, C. Liao, Y. Zou, Y. Zhang, Z. Kang, X. Yang, L. Wang, *J. Trauma Acute Care Surg.* **2011**, *70*, 1213.
- [6] M. Sever, E. Erek, R. Vanholder, G. Kantarci, M. Yavuz, A. Turkmen, H. Ergin, M. Tulbek, M. Duranay, G. Manga, *Clin. Nephrol.* **2003**, *59*, 326.
- [7] a) I. Najafi, W. Van Biesen, A. Sharifi, M. Hoseini, F. R. Farokhi, H. Sanadgol, R. Vanholder, *J. Nephrol.* **2008**, *21*, 776; b) U. Derici, O. Ozkaya, T. Arinsoy, D. Erbas, S. Sindel, M. Bali, N. Buyan, E. Hasanoglu, O. Soylemezoglu, *Clin. Chem. Acta* **2002**, *322*, 99.
- [8] C. Fenzl, M. Kirchinger, T. Hirsch, O. Wolfbeis, *Chemosensors* **2014**, *2*, 207.
- [9] J. Yin, Y. Hu, J. Yoon, *Chem. Soc. Rev.* **2015**, *44*, 4619.
- [10] H. Su, W. Ruan, S. Ye, Y. Liu, H. Sui, Z. Li, X. Sun, C. He, B. Zhao, *Talanta* **2016**, *161*, 743.
- [11] B. Zheng, F. Wang, S. Dong, F. Huang, *Chem. Soc. Rev.* **2012**, *41*, 1621.
- [12] a) M. R. Awual, T. Yaita, T. Taguchi, H. Shiwaku, S. Suzuki, Y. Okamoto, *J. Hazard. Mater.* **2014**, *278*, 227; b) J. Guo, J. Lee, C. I. Contescu, N. C. Gallego, S. T. Pantelides, S. J. Pennycook, B. A. Moyer, M. F. Chisholm, *Nat. Commun.* **2014**, *5*, 5389; c) S. Dong, B. Zheng, D. Xu, X. Yan, M. Zhang, F. Huang, *Adv. Mater.* **2012**, *24*, 3191; d) T. Terashima, M. Kawabe, Y. Miyabara, H. Yoda, M. Sawamoto, *Nat. Commun.* **2013**, *4*, 2321.
- [13] N. Schuwer, H. A. Klok, *Adv. Mater.* **2010**, *22*, 3251.
- [14] Z. Jarolímová, M. Vishe, J. Lacour, E. Bakker, *Chem. Sci.* **2016**, *7*, 525.
- [15] H. R. Yu, X. J. Ju, R. Xie, W. Wang, B. Zhang, L. Y. Chu, *Anal. Chem.* **2013**, *85*, 6477.
- [16] a) Z. Xue, S. Wang, L. Lin, L. Chen, M. Liu, L. Feng, L. Jiang, *Adv. Mater.* **2011**, *23*, 4270; b) V. Yesilyurt, M. J. Webber, E. A. Appel, C. Godwin, R. Langer, D. G. Anderson, *Adv. Mater.* **2016**, *28*, 86; c) A. S. Hoffman, *Adv. Drug Delivery Rev.* **2012**, *64*, 18; d) Z. Zhu, C. Wu, H. Liu, Y. Zou, X. Zhang, H. Kang, C. J. Yang, W. Tan, *Angew. Chem.* **2010**, *122*, 1070; e) M. V. Risbud, R. R. Bhonde, *Drug Delivery* **2000**, *7*, 69.
- [17] a) T. Yoshii, S. Onogi, H. Shigemitsu, I. Hamachi, *J. Am. Chem. Soc.* **2015**, *137*, 3360; b) F. Wang, J. Zhang, X. Ding, S. Dong, M. Liu, B. Zheng, S. Li, L. Wu, Y. Yu, H. W. Gibson, F. Huang, *Angew. Chem.* **2010**, *49*, 1090.
- [18] a) A. Giovannitti, C. B. Nielsen, J. Rivnay, M. Kirkus, D. J. Harkin, A. J. P. White, H. Sirringhaus, G. G. Malliaras, I. McCulloch, *Adv. Func. Mater.* **2016**, *26*, 514; b) Y. Inokuchi, T. Ebata, T. R. Rizzo, O. V. Boyarkin, *J. Am. Chem. Soc.* **2014**, *136*, 1815; c) G. Olsen, J. Ulstrup, Q. Chi, *ACS Appl. Mater. Interfaces* **2016**, *8*, 37.
- [19] J. R. Tse, A. J. Engler, *Current protocols in cell biology*, Wiley, Hoboken, NJ, USA **2010**.
- [20] R. Gref, A. Domb, P. Quellec, T. Blunk, R. Müller, J. Verbavatz, R. Langer, *Adv. Drug Delivery Rev.* **2012**, *64*, 316.
- [21] C. M. Hui, J. Pietrasik, M. Schmitt, C. Mahoney, J. Choi, M. R. Bockstaller, K. Matyjaszewski, *Chem. Mater.* **2013**, *26*, 745.
- [22] a) S. K. Vashist, P. Vashist, *J. Sens.* **2011**, *2011*, *1*; b) T. Zhou, K. A. Marx, M. Warren, H. Schulze, S. J. Braunhut, *Biotechnol. Prog.* **2000**, *16*, 268.
- [23] a) R. E. Speight, M. A. Cooper, *J. Mol. Recognit.* **2012**, *25*, 451; b) C. Yao, T. Zhu, Y. Qi, Y. Zhao, H. Xia, W. Fu, *Sensors* **2010**, *10*, 5859.
- [24] K. A. Marx, *Biomacromolecules* **2003**, *4*, 1099.
- [25] a) M. Lazerges, H. Perrot, N. Rabehagaso, C. Compere, *Biosensors* **2012**, *2*, 245; b) Y. Tsuge, Y. Moriyama, Y. Tokura, S. Shiratori, *Anal. Chem.* **2016**, *88*, 10744; c) D. D. Erbahr, I. Gürol, F. Zelder, M. Harbeck, *Sens. Actuators, B* **2015**, *207*, 297.
- [26] a) P. Miao, Y. Tang, B. Wang, K. Han, X. Chen, H. Sun, *Analyst* **2014**, *139*, 5695; b) G. Duner, H. Anderson, Z. Pei, B. Ingemarsson, T. Aastrup, O. Ramstrom, *Analyst* **2016**, *141*, 3993.
- [27] a) J. Zuo, E. Torres, *Langmuir* **2010**, *26*, 15161; b) M. Momeni, H. Saghafian, F. Golestani-Fard, N. Barati, A. Khanahmadi, *Appl. Surf. Sci.* **2017**, *392*, 80.
- [28] P. Vejayakumaran, I. A. Rahman, C. S. Sipaut, J. Ismail, C. K. Chee, *J. Colloid Interface Sci.* **2008**, *328*, 81.
- [29] M. Teresa, S. R. Gomes, K. S. Tavares, J. A. B. P. Oliveira, *Analyst* **2000**, *125*, 1983.
- [30] a) S. Ast, T. Schwarze, H. Muller, A. Sukhanov, S. Michaelis, J. Wegener, O. S. Wolfbeis, T. Korzdorfer, A. Durkop, H. J. Holdt, *Chem. - Eur. J.* **2013**, *19*, 14911; b) H. Zhang, I. H. Chu, S. Leming, D. V. Dearden, *J. Am. Chem. Soc.* **1991**, *113*, 7415; c) P. Nandhikonda, M. P. Begaye, M. D. Heagy, *Tetrahedron Lett.* **2009**, *50*, 2459.
- [31] L.-W. Xia, R. Xie, X.-J. Ju, W. Wang, Q. Chen, L.-Y. Chu, *Nat. Commun.* **2013**, *4*, 2226.
- [32] M. Rodahl, F. Höök, B. Kasemo, *Anal. Chem.* **1996**, *68*, 2219.